Nuclear Magnetic Resonance Investigations of Configurational Non-rigidity in Dinuclear Platinum(IV) Complexes. Part 4.† Ring Reversal, Pyramidal Inversion, and Novel Fluxional Rearrangements in $[(PtXMe_3)_2(MeSCH_2SeMe)]$ Complexes

By **Edward W. Abel, Kenneth Kite, Keith G. Orrell, Vladimir Šik,** and **Bruce L. Williams,** Department of Chemistry, University of Exeter, Exeter EX4 4QD

Dinuclear complexes of the type DL-$[(PtXMe_3)_2(MeSCH_2SeMe)]$ containing both Pt^{IV}–S and Pt^{IV}–Se bonds have been isolated. Detailed variable-temperature n.m.r. studies have established the existence of ligand ring reversal, pyramidal inversion of both S and Se atoms, ligand commutation (switching) between Pt atom pairs and scrambling of the platinum methyl environments which is considered to be a consequence of rapid ligand commutation producing a highly non-rigid seven-co-ordinate Pt^{IV} intermediate. Accurate energy barriers for these non-dissociative dynamic processes have been computed. Despite the probable non-synchronous nature of the S/Se double inversion, the spectra are shown to be sensitive only to Se inversion.

PREVIOUS studies[1-3] in this series have described the complexes formed by the reaction of $[(PtXMe_3)_4]$ with a variety of linear chalcogen ligands of the type L = $MeE(CH_2)_nEMe$ (E = S or Se, n = 0 or 1) and cyclic sulphur ligands of the type L = SCHRSCHRECHR (E = S or CH_2, R = H or Me). N.m.r. and X-ray studies have established that the complexes are dinuclear Pt^{IV} species $[(PtXMe_3)_2L]$ with a pair of halogen bridge bonds. Furthermore, between temperatures of *ca.* −100 °C and 100 °C n.m.r. studies have revealed a rich variety of conformational and configurational non-rigidity in these complexes. The most novel of these internal dynamic processes are the 1,3-switching[1,2] or 1,3-pivoting[3] of the ligand between the pairs of Pt atoms, and the scrambling of the Pt–Me environments. The spectral evidence for the ligand switching process in the complexes $[(PtXMe_3)_2\{MeE(CH_2)_nEMe\}]$, while fairly conclusive, involves only changes in ^{195}Pt–H coupling constants which lead to quite subtle changes in lineshape. In order to establish the existence of this ligand commutation with greater certainty we have now prepared analogous complexes with the mixed chalcogen ligand $MeSCH_2SeMe$. These complexes possess an advantage over the dithio- and diseleno-ether complexes in that the ligand switching process should in principle be detected by chemical-shift averaging of both the axial and equatorial Pt–Me signals. These mixed chalcogen ligand complexes also provide greater insight both into the mechanisms of the inversion and fluxional processes, and also into the question of whether the ligand switching and methyl scrambling phenomena should be viewed as independent fluxions or as consecutive aspects of a single fluxional rearrangement. This paper describes the variable-temperature n.m.r. evidence from which certain more definite conclusions on these matters can now be drawn.

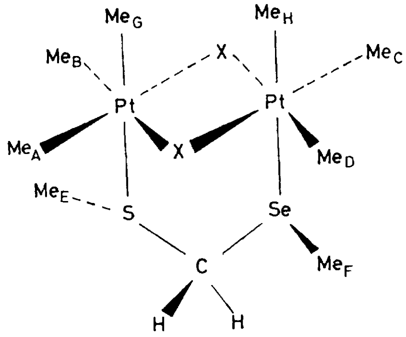

FIGURE 1 Structure of DL-$[(PtXMe_3)_2(MeSCH_2SeMe)]$ complexes

EXPERIMENTAL

Materials.—The following starting materials were prepared by literature methods as follows: dimethyl diselenide,[4] b.p. 153 °C (760 mmHg ‡); α-chloromethyl methyl sulphide,[5] b.p. 104—106 °C (760 mmHg). Trimethylplatinum(IV) iodide[6] was converted to trimethylplatinum sulphate,[7] and the other trimethylplatinum(IV) halides obtained by reaction of the latter with the appropriate potassium halide.[8]

Methylseleno(methylthio)methane.—This preparation was carried out under an atmosphere of dry nitrogen. Sodium metal (4.6 g, 0.20 mol) was added to liquid ammonia (500 cm^3) at −78 °C (acetone–CO_2 bath) over a period of 20 min. To this vigorously stirred, dark blue solution dimethyl diselenide (15.2 g, 0.08 mol) was added dropwise, and the mixture left stirring overnight to allow the ammonia to evaporate. Excess α-chloromethyl methyl sulphide (23.2 g, 0.24 mol) was added slowly to the residual solid and the reaction vessel was shaken vigorously to ensure efficient mixing. The suspension was then stirred at 50 °C for 24 h. Water (150 cm^3) and chloroform (150 cm^3) were added to dissolve the inorganic salt and organic liquid respectively. The layers were separated and the aqueous layer extracted with chloroform (2 × 100 cm^3). The combined organic layer and extracts were dried over magnesium sulphate, filtered, and the chloroform removed. The residual liquid was fractionally distilled under reduced pressure to yield the *product* as a yellow liquid, b.p. 60—61 °C (10 mmHg) (10.7 g, 73%). ^1H N.m.r.: δ (p.p.m.) 1.98 (Se–Me), 2.08 (S–Me), 3.58 (CH_2). The ligand contained a trace of

---

† Part 3 is ref. 3.

‡ Throughout this paper: 1 mmHg = (101 325/760) N m^{-2}.

MeSCH$_2$SMe which could not be removed by subsequent fractional distillation.

The preparations of the complexes were very similar and a representative method for the chloride complex is given.

Di-μ-chloro-hexamethyl-μ-(1-methylseleno-1-methylthiomethane)-diplatinum(IV).—To a solution of [(PtClMe$_3$)$_4$] (0.099 g, 0.36 mmol) in chloroform (5 cm^3) an excess of MeSCH$_2$SeMe (0.029 g, 0.37 mmol) in chloroform (2 cm^3) was added. The reaction mixture was stirred under reflux for 2 h and evaporated to dryness. Recrystallisation from hot chloroform–petroleum ether gave the *product* as shining white crystals (0.092 g, 73%).

TABLE 1

Characterisation of the dinuclear complexes

Complex	Colour	M.p./°C	Analysis */%	
			C	H
[(PtClMe$_3$)$_2$(MeSCH$_2$SeMe)]	White	210—212	15.30 (15.30)	3.65 (3.70)
[(PtBrMe$_3$)$_2$(MeSCH$_2$SeMe)]	White	188—190	13.80 (13.60)	3.20 (3.45)
[(PtIMe$_3$)$_2$(MeSCH$_2$SeMe)]	Yellow-white	150—152	12.45 (12.15)	2.85 (2.95)

* Calculated values in parentheses.

N.M.R. Spectra.—All the complexes were examined in CS$_2$–CD$_2$Cl$_2$ solvent mixtures for low-temperature studies (*ca.* −100 °C to ambient) and in CDCl$_3$ for above-ambient studies. All ^{1}H spectra were recorded at 100 MHz using a JEOL PS/PFT-100 spectrometer equipped with a standard variable-temperature accessory. Temperature measurements were made with a Comark digital thermometer (Type 5000) based on a Cu/Cu–Ni thermocouple. Bandshape analyses were carried out using our modified version of the original DNMR program of Kleier and Binsch.[9] Computer simulated spectra were fitted visually and energy parameters, derived from the standard Arrhenius and Eyring plots, are based on least-squares fittings of at least 8 data points. The errors quoted for the free energies of activation $\Delta G^{\ddagger}$ are based on the numerical difference between the standard deviations of $\Delta H^{\ddagger}$ and $T\Delta S^{\ddagger}$ (where T = 298.15 K) following the practice of Binsch and Kesser.[10] In this way, the relatively low sensitivity of $\Delta G^{\ddagger}$ to systematic error is most realistically expressed.

RESULTS

Properties of the Complexes.—The complexes, prepared as described above, are white or pale yellow crystalline solids which are readily soluble in organic solvents and are stable both in air and in solution. Analytical data, given in Table 1, are consistent with the dinuclear structures (Figure 1). N.m.r. spectra showed that the complexes were formed with ease, the reactions being virtually complete within 1 h, and with no by-products formed.

Low-temperature N.M.R. Studies.—The three complexes [(PtXMe$_3$)$_2$(MeSCH$_2$SeMe)] (X = Cl, Br, or I) showed similar spectral features and the complex (X = Br) will be taken as typical. At *ca.* −79 °C the methyl protons produce well resolved lines (Figure 2) whereas the methylene region is rather less well resolved owing to second-order features. The methyl region consists of eight distinct signals (plus ^{195}Pt satellites) which are assigned to the chalcogen methyls (E, F), the axial platinum methyls (G, H), and the equatorial platinum methyls (A, B, C, D) as assigned in the spectrum (Figure 2) and labelled according to the proposed structure (Figure 1). This structure is analogous to that proposed for the dithio- and diseleno-ether complexes,[1,2,11,12] and is fully supported by the present spectrum at −79 °C, providing that a rapid reversal of the –S–CH$_2$–Se– portion of the six-membered ring is assumed. Lowering the temperature further caused the methyl and methylene signals to broaden. At *ca.* −107 °C the ligand methyls had coalesced and by *ca.* −117 °C they had sharpened somewhat to reveal four chemically shifted signals (Figure 2). Assuming two of these signals are due to S–Me and two to Se–Me protons the spectrum reveals the presence of the two possible DL structures having the ligand methyls mutually *trans* (Figure 3).

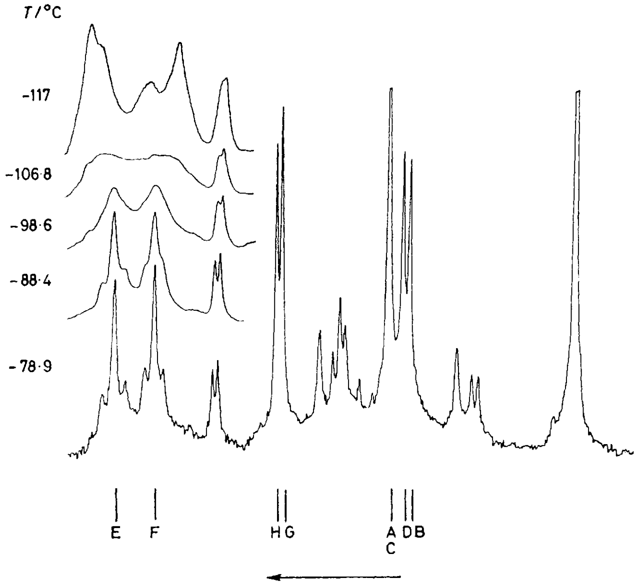

FIGURE 2 Low-temperature spectra (methyl region) of [(PtBrMe$_3$)$_2$(MeSCH$_2$SeMe)]. Labelling of lines in accordance with Figure 1. The changes in the chalcogen methyl signals E, F on cooling to −117 °C are due to a slowing of the reversal of the –S–CH$_2$–Se– portion of the ring

On warming the sample from *ca.* −79 °C the spectra show little change until *ca.* −40 °C when broadening of the equatorial Pt–Me signals commences. Coalescence occurs at *ca.* −25 °C and by *ca.* 0 °C the absorption envelope has sharpened to essentially a single line (Figure 4). On close inspection a slight shoulder on this absorption can be discerned indicating two averaged equatorial Pt–Me shifts with a very small chemical shift distinction between them. In addition, this band unfortunately overlaps with a small impurity band due to the complex [(PtBrMe$_3$)$_2$-(MeSCH$_2$SMe)]. Whilst this impurity interfered somewhat with the bandshape fitting procedures, it did not introduce any major source of error. The methylene region changed to a septet of lines by *ca.* 0 °C, this pattern being attributed to the pair of chemical-shift averaged protons coupling equally to the pair of ^{195}Pt atoms and to the ^{77}Se atom.

These spectral changes are clearly associated with pyramidal inversion of the S and Se atoms by analogy with the dithio- and diseleno-ether complexes.[1] This double inversion process causes averaging between the equatorial Pt–Me pairs A and B, and between C and D, leading to two averaged shifts which are just resolvable. The energy barriers associated with this process were assessed by simulating spectra based on $A \rightleftharpoons B$ and $C \rightleftharpoons D$ spin interconversions, making allowance in the usual way for ^{195}Pt satellite spectra. The ' best fit ' spectra are shown alongside the experimental spectra in Figure 4. These theoretical spectra were computed using the same rate constant for both $A \rightleftharpoons B$ and $C \rightleftharpoons D$ exchanges. This, however, does *not* necessarily imply that S and Se inversion energies are the same. We will show in the Discussion section that since the spectra are only sensitive to inversions of *both* chalcogens then, if the two energy barriers are different, only the higher barrier will be measurable. The static parameters used in the bandshape fittings are given in Table 2 and the inversion energies in Table 3.

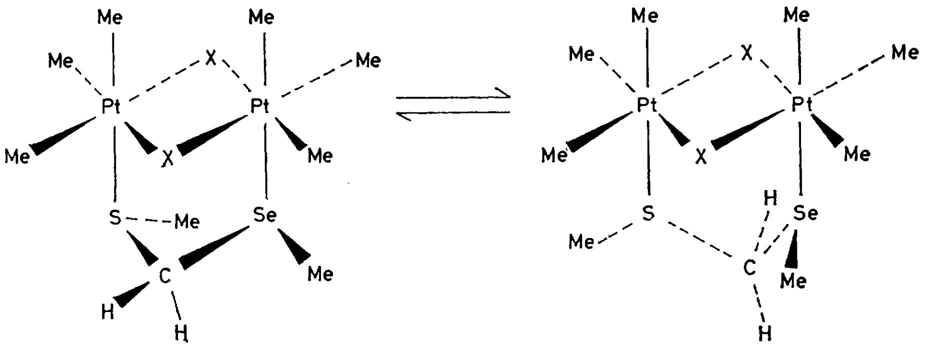

FIGURE 3 The two static DL conformers of [$(PtXMe_3)_2(MeSCH_2SeMe)$]

TABLE 2

Static parameters used in calculating the pyramidal inversion energies †

Complex	ν_A	$^2J(AX)$	ν_B	$^2J(BX)$	ν_C	$^2J(CX)$	ν_D	$^2J(DX)$	T_2^*/s
[$(PtClMe_3)_2(MeSCH_2SeMe)$]	94.0	77.6	81.5	77.1	93.1	77.1	84.8	77.4	0.367
[$(PtBrMe_3)_2(MeSCH_2SeMe)$]	109.9	75.9	96.7	76.4	108.6	75.9	100.6	76.9	0.183
[$(PtIMe_3)_2(MeSCH_2SeMe)$]	126.5	74.2	112.9	74.6	123.7	74.0	117.3	75.2	0.200

† Chemical shifts and coupling constants (both in Hz) measured at low temperatures, shifts relative to $SiMe_4$; solvent was $CDCl_3$.

High-temperature N.M.R. Studies.—At temperatures well above those where S/Se inversion was fast on the n.m.r. time scale, all the complexes were observed to undergo additional configurational changes. These changes, studied in the approximate range 0—85 °C, were perfectly reversible and non-dissociative in nature since ^{195}Pt–H (ligand proton) couplings were retained. These changes which affected both the E–Me and Pt–Me regions are attributable to 180° switching of the ligand between the Pt atom pairs and to platinum methyl scrambling as described previously.[1]

Intermetallic Ligand Switching.—Both the S–Me and Se–Me signals changed from triplets (1 : 4 : 1) to quintets (1 : 7.8 : 17.5 : 7.8 : 1) with an approximate halving of the ^{195}Pt–H couplings (Figure 5). In addition, the two axial Pt–Me signals (G, H) and the two averaged equatorial Pt–Me signals (⟨AB⟩, ⟨CD⟩) each coalesced to single lines with ^{195}Pt satellites. The lineshape changes of the E–Me region were computed for the various subspectra associated with the different ^{195}Pt and ^{77}Se isotopic species as described for the dithio- and diseleno-analogues. The results are shown in Figure 5 and are based on the static parameters in Table 4.

Intramolecular Platinum Methyl Scrambling.—At the onset of ligand switching, the Pt–Me signals broadened and eventually coalesced to a singlet (plus ^{195}Pt satellites) (Figure 6). The energy of this associated methyl scrambling process was computed as follows.

At *ca.* 6 °C when inversion was rapid but both fluxional processes slow, the four signals in the Pt–Me region were assigned as shown below. The ligand switching causes the interconversions $1 \rightleftharpoons 2$, $3 \rightleftharpoons 4$ and the methyl scrambling produces $1 \rightleftharpoons 3$, $2 \rightleftharpoons 4$. As no Me–Me spin couplings were detected the spin problem is of the type shown. The populations of the configurations H, G,

TABLE 3

Energy parameters for double chalcogen inversion in [$(PtXMe_3)_2L$] complexes

L	X	E_a/kJ mol^{-1}	$\log_{10} A$	$\Delta G^\ddagger$/kJ mol^{-1}	$\Delta H^\ddagger$/kJ mol^{-1}	$\Delta S^\ddagger$/J K^{-1} mol^{-1}
$MeSCH_2SMe$	Cl	40.6 ± 3.1	11.4 ± 0.8	48.5 ± 1.6	38.9 ± 3.1	−32.0 ± 15.6
	Br	48.9 ± 2.4	13.5 ± 0.6	44.6 ± 1.1	47.2 ± 2.4	8.7 ± 11.8
$MeSeCH_2SeMe$	Cl	62.0 ± 2.7	13.8 ± 0.6	56.3 ± 0.4	59.9 ± 2.7	11.9 ± 10.5
	Br	55.9 ± 3.0	12.6 ± 0.6	57.7 ± 0.4	53.8 ± 3.0	−10.9 ± 11.5
$MeSCH_2SeMe$	Cl	57.4 ± 0.6	13.2 ± 0.1	55.3 ± 0.1	55.2 ± 0.6	−0.3 ± 2.1
	Br	58.0 ± 1.8	13.4 ± 0.4	54.5 ± 0.3	55.9 ± 1.8	5.1 ± 6.8
	I	52.2 ± 1.5	12.1 ± 0.3	56.0 ± 0.3	50.1 ± 1.5	−20.0 ± 6.0

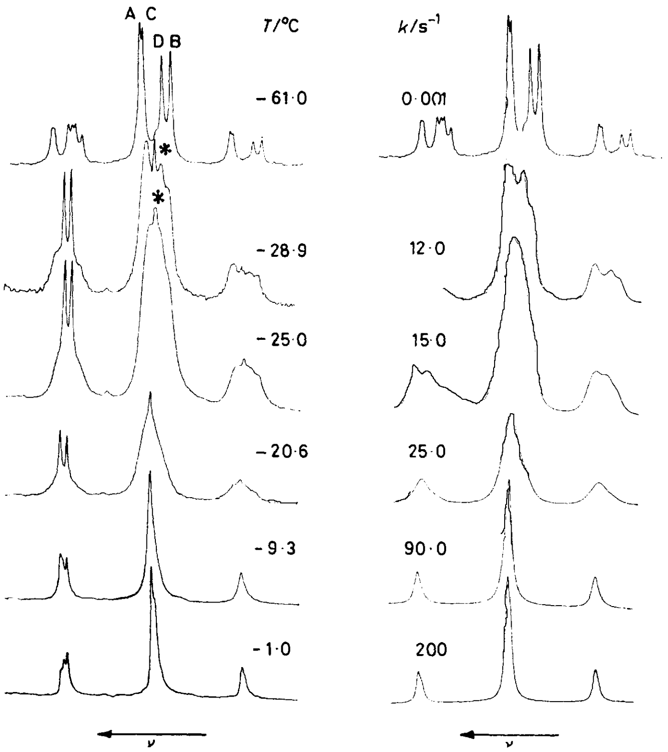

FIGURE 4 Experimental and computer synthesised spectra (platinum methyl region) of $[(PtBrMe_3)_2(MeSCH_2SeMe)]$ showing the effects of chalcogen inversion. The band marked (*) is due to a trace of $[(PtBrMe_3)_2(MeSCH_2SMe)]$

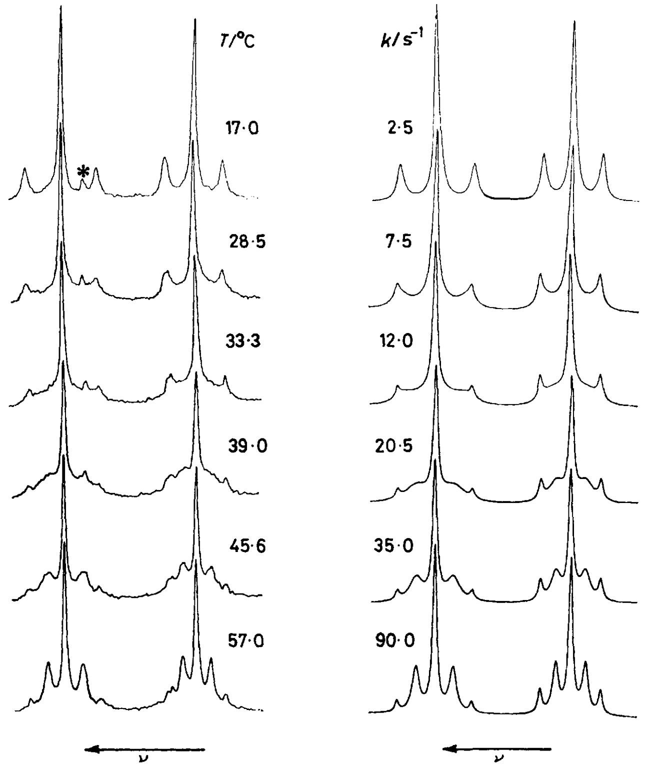

FIGURE 5 Experimental and computer synthesised spectra (chalcogen methyl region) of $[(PtBrMe_3)_2(MeSCH_2SeMe)]$ showing the effects of ligand switching. The band marked (*) is due to a trace of $[(PtBrMe_3)_2(MeSCH_2SMe)]$

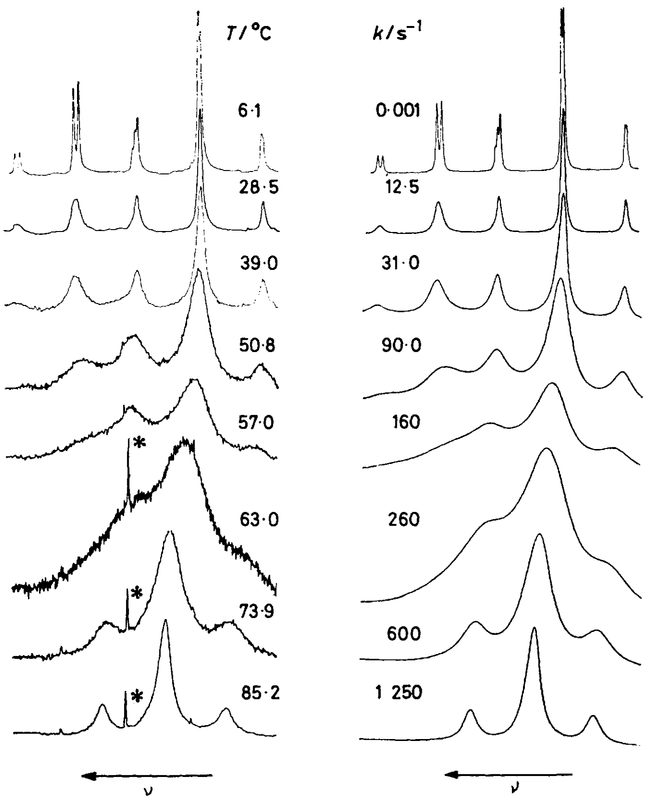

FIGURE 6 Experimental and computer synthesised spectra (platinum methyl region) of $[(PtBrMe_3)_2(MeSCH_2SeMe)]$ showing the effects of platinum methyl scrambling. The band marked (*) in the higher temperature spectra is due to some $[(PtBrMe_3)_4]$ produced by dissociation

⟨AB⟩, ⟨CD⟩ are in the ratio 1 : 1 : 2 : 2 and the static parameters are given in Table 5. Owing to the similarity of shifts of the axial methyls H and G, and of the averaged equatorial methyl pairs ⟨CD⟩ and ⟨AB⟩, the spectra were found to be insensitive to the ligand switching rate constants k_{12} and k_{34}. The values of these rate constants were therefore taken from the E–Me fittings and the Pt–Me region was used to calculate only the methyl scrambling energies. Experimental and theoretical spectra are shown in Figure 6.

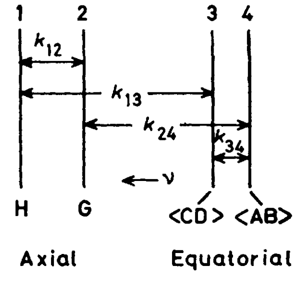

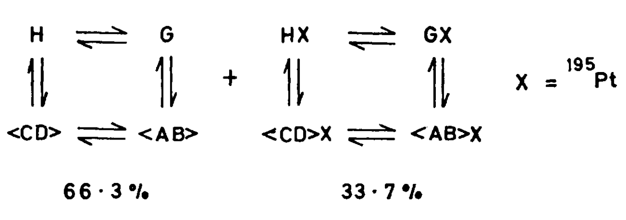

TABLE 4

Static parameters used in calculating ligand switching energy barriers †

Complex	ν_E	^3J(EX)	ν_F	^3J(FX)	^2J(SeMe)	T_2^*/s
$[(PtClMe_3)_2(MeSCH_2SeMe)]$	250.5	11.9	231.6	9.0	9.4	0.353
$[(PtBrMe_3)_2(MeSCH_2SeMe)]$	254.3	12.3	231.9	9.8	10.0	0.400
$[(PtIMe_3)_2(MeSCH_2SeMe)]$	260.2	12.8	233.8	10.2	10.2	0.250

† Chemical shifts (relative to $SiMe_4$) and coupling constants measured in Hz; solvent was $CDCl_3$.

DISCUSSION

Ring Reversal and Pyramidal Inversion.—In the present mixed chalcogen complexes it was not possible to fully retard the reversal of the $-S-CH_2-Se-$ part of the six-membered ring and therefore an accurate energy barrier could not be computed. However, from line broadening effects between *ca.* −80 °C and −120 °C the barrier is estimated to be *ca.* 40 kJ mol^{-1} for the complex (X = Cl). This value is lower than that found for the dithio-analogue ($\Delta G^{\ddagger} = 44.8 \pm 0.7$ kJ mol^{-1}) and higher than that predicted (30—40 kJ mol^{-1}) for the diseleno-analogue where no line broadening effects were observed. Such a trend in values is in keeping with results found for six-membered chalcogen heterocycles, where the ring reversal barrier depends primarily on the magnitude of the C–E torsional barriers.[13] Microwave studies have indicated that C–Se torsional barriers are lower than C–S barriers.[14] This observation is consistent with the $\Delta G^{\ddagger}$ values of 34.3 [15] and 43.1 kJ mol^{-1} [16] quoted for ring reversal barriers of $\overline{\mathrm{ECH_2ECH_2CH_2C}}\mathrm{H_2}$ where E = Se and S, respectively.

The energy data associated with the double chalcogen inversion process are given in Table 3 where these new data are compared with those of the dithio- and diseleno-analogues. Of immediate note is the listing of only one set of energy parameters for the mixed S/Se ligand complexes. By comparison with the diselenoether complexes we are confident the data refer to the Se atom inversion barrier, but are uncertain as to the magnitude of the S atom inversion (see below).

Pyramidal inversion of atom pairs may proceed by 3 possible mechanisms,[17] namely (i) uncorrelated (*i.e.* independent) inversion of each atom, (ii) correlated non-simultaneous inversion of both atoms, and (iii) synchronous inversion of both atoms. In the case of identical chalcogen atom pairs we have argued in Part 2 (ref. 2) in favour of mechanism (ii). In the present mixed chalcogen systems the actual mechanism operating is still not unambiguously settled but a non-synchronous process would appear more likely from the following analysis.

Since ring reversal is fast on the n.m.r. time scale at the temperature of onset of pyramidal inversion a pseudo-planar $-S-CH_2-Se-$ fragment can be assumed and double inversion involves (1) $\rightleftharpoons$ (1′) (below). Synchronous inversion would proceed *via* the transition-state structure (2) with planar sp^2 hybridised S and Se atoms. Non-simultaneous inversion will require the transition-state structures (3) and (5), and the DL invertomer (4); the two mechanisms can be summarised as shown. The energy profiles for these two schemes are shown below where it is assumed the inversion barrier at Se is greater than at S: synchronous (· · ·) and non-synchronous (——) processes.

TABLE 5

Static parameters used in calculating the platinum methyl scrambling energy barriers [a]

	Axial Pt-Me				Equatorial Pt-Me				
Complex	ν_G	^2J(GX)	ν_H	^2J(HX)	$\nu_{\langle AB\rangle}$ [b]	$^2J\langle AB\rangle$	$\nu_{\langle CD\rangle}$	$^2J\langle CD\rangle$	T_2^*/s
$[(PtClMe_3)_2(MeSCH_2SeMe)]$	161.0	70.8	164.3	70.5	93.2	76.9	94.8	77.2	0.25
$[(PtBrMe_3)_2(MeSCH_2SeMe)]$	176.8	71.1	179.7	71.1	102.5	76.7	103.8	76.7	0.27
$[(PtIMe_3)_2(MeSCH_2SeMe)]$	207.1	72.6	209.1	72.5	118.9	74.2	119.6	74.2	0.27

[a] Chemical shifts (relative to $SiMe_4$) and coupling constants measured in Hz; solvent was $CDCl_3$. [b] $\nu\langle AB\rangle$ represents the chemical shift of the dynamic averaged A and B signals, *etc.*; comparison with Table 2 shows the appreciable temperature dependence of these shifts.

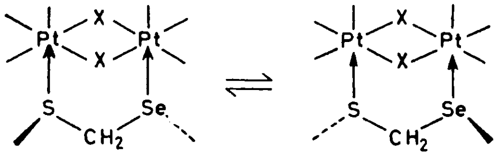

(1) (1′)

The failure to detect the DL invertomer (4) means that, if the double inversion is non-simultaneous, the S inversion barrier is not separately detectable and n.m.r. lineshapes will be sensitive only to the Se barrier because this is the rate-limiting stage of the double inversion (1) $\rightleftharpoons$ (1′) process. If the double inversion is synchronous then the S and Se barriers will be identical. Preference for either of these processes based on purely spectral evidence is, however, difficult to ascertain. We have shown that in the dithio- and diseleno-ether complexes the inversion barriers at S are invariably lower than the corresponding barriers at Se. If the process is non-simultaneous, S inversion should become rapid in n.m.r. terms before Se inversion gets underway.

In contrast, a synchronous double-inversion mechanism implies that non-bonded E–Me ··· Me–E interactions are the dominant cause of the normally faster S inversion being held back until the Se inversion commences, after which the two inversions become synchronous. A clear distinction between these two mechanisms requires knowledge of the relative energies of the intermediates (2) and (5). In the absence of estimates of these quantities the actual mechanism of the double inversion process remains in some doubt. We are currently examining the possibilities of semi-empirical molecular orbital calculations in this context, since extended Hückel type calculations have recently been applied with considerable success to other platinum complexes.[18,19]

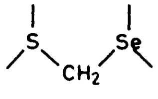
(2)

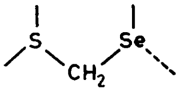
(3)

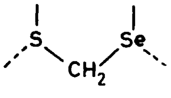
(4)

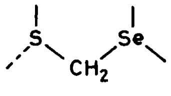
(5)

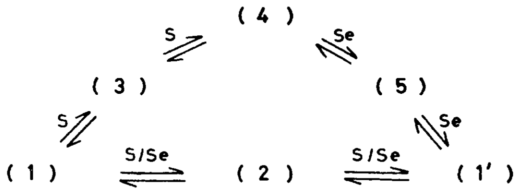

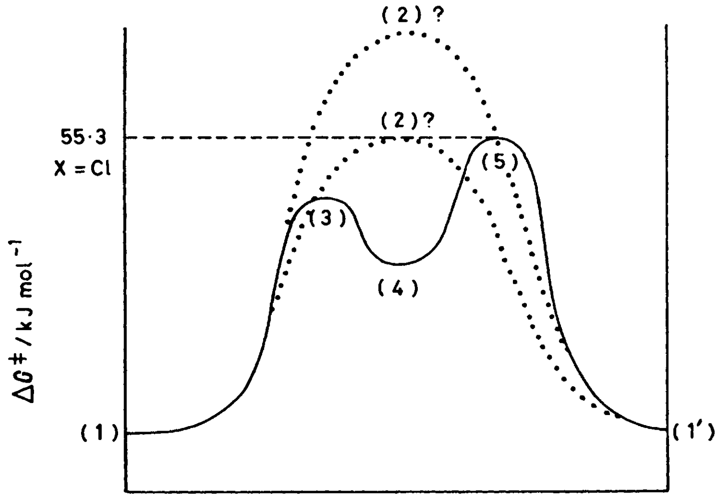

Ligand Switching and Platinum Methyl Scrambling.—The energy data for these processes are collated in Table 6 where it will be seen that the data for the two fluxions are almost equal within experimental error. This reinforces our earlier suggestion [2] that the two processes are not separable, since the ligand switching motion may be visualised as proceeding *via* an intermediate which initiates the methyl scrambling. Before considering questions of mechanism, however, we will discuss some factors which appear to influence the energy barriers of these processes.

Inspection of the activation parameters in Table 6, and in particular the $\Delta G^{\ddagger}$ values which are least prone to systematic error, shows a dependence on ring size, and on the chalcogen and halogen atoms. The ring size dependence can be expressed in terms of the angle between the Pt–E bond and the Pt · · · Pt plane, and the direct E · · · E bite distance. The greater the ring strain in the ground-state configuration, the more likely it is that this strain will be relieved in the transition-state structure(s), resulting in a smaller difference between ground- and excited-state energies compared to complexes with less strained rings. In this way the significantly lower switching barriers for five-membered ring complexes compared to their six-membered analogues can be rationalised. The data also show that the switching barrier is lowered by lighter donor atoms (*i.e.* S rather than Se) and by heavier halogens.

The halogen dependence requires further discussion. The coupling-constant data in Table 2 show that the ^{2}J(Pt–H) values for methyls *trans* to halogen decrease with halogen such that $\mathrm{Cl} > \mathrm{Br} > \mathrm{I}$ with a subsequent increase in ^{2}J(Pt–H) values for methyls *cis* to halogen (Table 5). This trend implies a redistribution of electron density around the Pt atoms such that the Pt–X bonds are strengthened on increasing halogen size. If the ligand switching commutation initiates halogen bridge bond breaking and the formation of a highly fluxional five-co-ordinate $\mathrm{Pt^{IV}}$ species, then the methyl scrambling energy is expected to *increase* significantly with halogen size, whereas the reverse trend is observed. Moreover, examination of ^{3}J(Pt–H) data (Table 4) shows an increase in the coupling in the order $\mathrm{Cl} < \mathrm{Br} < \mathrm{I}$, which implies a shortening of the Pt–E bonds and thereby aiding the chalcogen lone pairs in switching their donation from one Pt atom to the other.

It is clear that the trend in the ^{3}J(Pt–H) data is consistent with the observed halogen dependences of the $\Delta G^{\ddagger}$ values for ligand switching and methyl scrambling.

TABLE 6

Energy parameters for ligand switching and methyl scrambling in $[(PtXMe_3)_2L]$ complexes

L	Process	X	E_a/kJ mol^{-1}	$\log_{10} A$	$\Delta G^{\ddagger}$/kJ mol^{-1}	$\Delta H^{\ddagger}$/kJ mol^{-1}	$\Delta S^{\ddagger}$/J K^{-1} mol^{-1}
MeSSMe	Switching	Cl	61.3 ± 3.9	12.8 ± 0.7	61.3 ± 0.4	59.0 ± 3.9	-7.8 ± 14.2
	Scrambling	Cl	68.2 ± 2.0	13.8 ± 0.4	62.4 ± 0.2	65.8 ± 2.0	11.6 ± 7.2
MeSeSeMe	Switching	Cl	70.9 ± 3.8	13.8 ± 3.8	65.1 ± 0.1	68.5 ± 3.8	11.6 ± 12.8
	Scrambling	Cl	70.8 ± 2.4	13.8 ± 0.4	65.2 ± 0.1	68.3 ± 2.4	10.6 ± 8.0
MeSeSeMe	Switching	Br	71.5 ± 3.0	14.0 ± 0.5	64.5 ± 0.1	69.1 ± 3.1	15.5 ± 10.5
	Scrambling	Br	67.0 ± 2.3	13.2 ± 0.4	64.5 ± 2.2	64.6 ± 2.4	0.1 ± 0.8
MeSCHMeSMe	Switching	Cl	73.0 ± 2.2	13.1 ± 0.4	71.5 ± 0.3	70.2 ± 2.2	4.2 ± 6.6
	Scrambling	Cl	70.8 ± 3.9	12.7 ± 0.6	71.6 ± 0.5	67.9 ± 3.9	-12.2 ± 11.5
MeSeCHMeSeMe	Switching	Cl	70.8 ± 7.8	12.5 ± 1.2	72.6 ± 6.8	68.0 ± 7.8	-11.6 ± 3.5
	Scrambling	Cl	71.5 ± 3.5	12.6 ± 0.5	72.8 ± 0.4	68.7 ± 3.5	-14.0 ± 10.3
$MeSCH_2SeMe$	Switching	Cl	60.7 ± 0.3	11.3 ± 0.1	69.5 ± 0.1	58.1 ± 0.3	-39.2 ± 0.8
	Scrambling	Cl	80.4 ± 0.8	14.6 ± 0.1	70.3 ± 0.1	77.6 ± 0.8	24.5 ± 2.4
$MeSCH_2SeMe$	Switching	Br	71.4 ± 0.4	13.3 ± 0.1	68.8 ± 0.1	68.8 ± 0.4	0.1 ± 1.3
	Scrambling	Br	73.6 ± 0.7	13.8 ± 0.1	67.6 ± 0.1	70.9 ± 0.7	10.8 ± 2.2
$MeSCH_2SeMe$	Switching	I	58.5 ± 1.1	11.5 ± 0.2	65.6 ± 0.1	56.0 ± 1.0	-31.2 ± 3.6
	Scrambling	I	70.1 ± 0.4	13.7 ± 0.1	64.8 ± 0.1	67.4 ± 0.4	8.7 ± 1.2

In contrast, if halogen bridge bonds actually break and reform during the scrambling process, the ^2J(Pt–H) values predict a halogen dependence which is *opposite* to that actually observed. In view of these new data we do not now feel it either necessary or indeed correct to invoke a scrambling mechanism involving a random cleavage of the halogen bridge bonds to form a highly fluxional five-co-ordinate Pt^{IV} complex as we suggested previously.[1,2] Instead, we propose that an intermediate which is formed as a result of the ligand moving through 90° from its ground-state configuration and having the chalcogen lone pairs weakly bonded to both Pt atoms (Figure 7) is itself the initiator of the scrambling of the axial and equatorial Pt–Me environments which will then necessarily occur at a rate comparable to that of ligand switching.

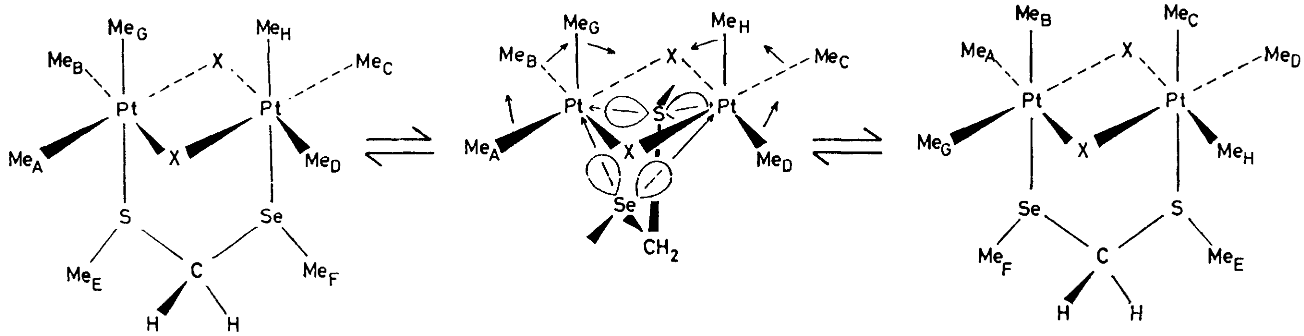

FIGURE 7 Proposed structure of the seven-co-ordinate Pt^{IV} intermediate of the ligand commutation process

It is also significant that methyl scrambling is not directly initiated as a result of the ligand pivots in the trithian complexes[3] but occurs only when the complex dissociates producing a five-co-ordinate Pt^{IV} species. In other words, halogen bridge breaking is not necessary to explain Pt–Me scrambling. The ligand pivot and methyl scrambling processes are clearly quite separate phenomena in these cyclic ligand complexes. In these latter complexes the intermediate of the ligand commutation process is likely to be a relatively stable species involving a normal six-co-ordinate Pt^{IV} atom and a seven-co-ordinate Pt^{IV} involving lone-pair donation from two suitably situated S atoms. It is, therefore, not surprising that the methyl scrambling does not occur at this stage. In the present complexes with the $MeSCH_2SeMe$ ligand the intermediate (Figure 7) involves two seven-co-ordinate Pt^{IV} atoms. Seven-co-ordinate species are highly stereochemically non-rigid[20] as has been predicted theoretically and semi-empirically, and confirmed experimentally by n.m.r. spectroscopy. It is, therefore, to be expected that the transient formation of the seven-co-ordinate species (Figure 7) will induce a rearrangement of the platinum methyl environments.

We are, therefore, inclined to the view that in these dinuclear Pt^{IV} complexes with linear chalcogen ligands the ligand switching and platinum-methyl scrambling processes are correlated phenomena and represent consecutive aspects of a single intramolecular fluxional rearrangement.

We thank Dr. Martin Booth for invaluable and stimulating discussions.

[1/723 *Received, 6th May,* 1981]

REFERENCES

[1] E. W. Abel, A. R. Khan, K. Kite, K. G. Orrell, and V. Šik, *J. Chem. Soc., Dalton Trans.*, 1980, 2208.
[2] E. W. Abel, A. R. Khan, K. Kite, K. G. Orrell, and V. Šik, *J. Chem. Soc., Dalton Trans.*, 1980, 2220.
[3] Part 3, E. W. Abel, M. Booth, G. King, K. G. Orrell, and V. Šik, *J. Chem. Soc., Dalton Trans.*, 1981, 1846.
[4] L. Brandsma and E. Wijers, *Recl. Trav. Chim.*, 1963, **82**, 68.
[5] F. G. Bordwell and B. H. Pitt, *J. Am. Chem. Soc.*, 1955, **77**, 572.
[6] J. C. Baldwin and W. C. Kaska, *Inorg. Chem.*, 1975, **14**, 2020.

[7] D. E. Clegg and J. R. Hall, *Spectrochim. Acta*, 1965, **21**, 357.

[8] D. E. Clegg and J. R. Hall, *J. Organomet. Chem.*, 1970, **22**, 491.

[9] D. A. Kleier and G. Binsch, DNMR3 Program 165, Quantum Chemistry Program Exchange, Indiana University, 1970.

[10] G. Binsch and H. Kessler, *Angew. Chem. Int. Ed.*, 1980, **19**, 411.

[11] E. W. Abel, A. R. Khan, K. Kite, K. G. Orrell, and V. Šik, *J. Organomet. Chem.*, 1978, **148**, C18.

[12] E. W. Abel, A. R. Khan, K. Kite, K. G. Orrell, and V. Šik, *J. Chem. Soc., Dalton Trans.*, 1980, 1169.

[13] J. B. Lambert and S. I. Featherman, *Chem. Rev.*, 1975, **75**, 611.

[14] J. B. Lambert, C. E. Mixan, and D. H. Johnson, *J. Am. Chem. Soc.*, 1973, **95**, 4634.

[15] A. Geens, G. Swaelens, and M. Anteunis, *Chem. Commun.*, 1969, 439.

[16] H. Friebolin, H. G. Schmid, S. Kabuss, and W. Faisst, *Org. Magn. Reson.*, 1969, **1**, 67.

[17] J. E. Anderson and J. M. Lehn, *J. Am. Chem. Soc.*, 1967, **89**, 81.

[18] D. M. P. Mingos, *J. Chem. Soc., Dalton Trans.*, 1977, 602.

[19] D. M. P. Mingos and C. R. Nurse, *J. Organomet. Chem.*, 1980, **184**, 281.

[20] E. L. Muetterties, *Acc. Chem. Res.*, 1970, **3**, 266.